

**Functional consequences of microRNA regulation by
polycyclic aromatic hydrocarbons in 3D human bronchial
epithelial cells**

By

Michael-Andres Dominic Mans

An Undergraduate Thesis Submitted to

Oregon State University

In partial fulfillment of
the requirements for the
degree of

Baccalaureate of Science in BioResource Research,
Genomics/Bioinformatics Option

09/12/2018

APPROVED:

Susan C. Tilton, Environmental and Molecular Toxicology

Date

David Williams, Environmental and Molecular Toxicology

Date

Katharine G. Field, BRR Director

Date

© Copyright by Michael-Andres Mans, 09/12/2018

I understand that my project will become part of the permanent collection of the Oregon State University Library, and will become part of the Scholars Archive collection for BioResource Research. My signature below authorizes release of my project and thesis to any reader upon request.

Michael-Andres Dominic Mans

Date

Abstract

Polycyclic aromatic hydrocarbons (PAHs) are a class of contaminants ubiquitous in the environment and result from the incomplete combustion of fossil fuels. Many PAHs have been identified as procarcinogenic, and are metabolized to form DNA adducts; however, other mechanisms also may contribute to toxicity and help explain differences in toxicity across the wide class of compounds. This study examines the role of microRNAs (miRNAs) in mediating toxicity by benzo[a]pyrene (BAP) and dibenzo[def,p]chrysene (DBC) in 3D human bronchial epithelial cells (HBEC). miRNAs are short (≤ 22 nt), non-coding RNA molecules that post-transcriptionally regulate gene expression. Recent studies have identified dysregulation of miRNA expression in response to BAP, cigarette smoke, and pollution-related lung diseases and cancers.

The 3D HBEC model provides a more accurate representation of the effects of PAH toxicity because it is metabolically competent, containing multiple cell types in a pseudostratified model that is more representative of in vivo exposure. This study aims to understand the functional consequences of miRNAs in HBEC after exposure to BAP and DBC, which have previously been found to function through unique mechanisms. Cells were exposed to 500 ug/ml BAP and 10 ug/ml DBC for 48 hrs and samples were collected for RNA isolation and parallel analysis of mRNA and miRNA by RNA sequencing using Illumina HiSeq 3000.

Significant ($q < 0.05$) differentially expressed miRNA and mRNA were analyzed in an anti-correlated fashion in Bioinformatics Resource Manager to identify miRNA-mRNA interactions and visualized as networks in Cytoscape to identify patterns of regulation

reflecting a response to PAHs. DBC treatments showed more regulation of unique miRNA, with 53 significantly down- and 46 up-regulated miRNAs, compared to BAP's 14 down- and 35 up-regulated miRNAs. These miRNAs targeted 546 up- and 654 down-regulated genes significant in the DBC dataset, and 176 up- and 750 down-regulated in the BAP. miRNAs uniquely up-regulated in BaP were linked with a more significant response in cell adhesion and developmental processes. In DBC, up-regulated miRNAs showed more significant response overall in regulation of cell cycle, translation, and apoptosis. Processes perturbed by down-regulated miRNA were less consistent, with BaP showing more effect for cytoskeletal and cell cycle processes, while DBC shows more response for cell adhesion and DNA damage. These data are the first to describe the role of miRNAs as regulators of PAH toxicity in primary human 3D HBEC and could represent important mechanisms associated with PAH-mediated lung disease and cancer in humans.

Introduction

Polycyclic aromatic hydrocarbons (PAHs) are ubiquitous contaminants in the environment that are composed of two or more aromatic rings and result from processing of food (e.g. grilling, smoking, and roasting,) or the incomplete combustion of organic material (e.g., diesel exhaust, coal tar, wood, tobacco, etc.) As such, non-smokers are primarily exposed to PAHs through diet or inhalation of pollutants (Choi 2010). Many PAHs are procarcinogenic and can lead to tumor development by causing damage directly to DNA. PAHs may also influence carcinogenesis via non-genotoxic pathways; however, those mechanisms are not yet clear. Lung cancer is the leading cause of cancer death among men and women and is the second most common form in new cancer cases and accounts for about a quarter of cancer deaths in the United States (Siegel et al., 2017.) Many PAHs and PAH metabolites are a concern because of their carcinogenic potential, however damage to the kidneys, liver, and blood have been observed as long-term health effects of naphthalene exposure, a two-benzene ring PAH (ATSDR, 2005.) Epidemiological studies have also linked PAH exposure in utero with impacted neurological development and fetal growth (ATSDR, 1995.)

Polycyclic Aromatic Hydrocarbons

Two PAHs of interest for this study are benzo[a]pyrene (BaP) and dibenzo[def,p]chrysene (DBC), which co-occur in environmental exposures and are both known to be procarcinogenic. PAHs are known to activate the aryl hydrocarbon receptor (AhR) as a transcription factor affecting downstream gene expression and translocating the PAH across the nuclear membrane; however, the mechanisms for carcinogenicity are not fully understood (Harper 2015). PAHs are metabolically activated by Cytochrome P4501A1 and epoxide hydrolase to form carcinogenic diol epoxides, which can interact with DNA; however, PAHs may also influence gene expression through non-genotoxic pathways.

miRNA

miRNAs are a form of post transcriptional regulation and may have an important role in regulating PAH-mediated toxicity. They are short non-coding RNA molecules that act to regulate gene expression by binding to target transcripts preventing synthesis of, or modifying, the final protein product. In healthy cells, miRNAs are involved in the normal function of cells by balancing gene expression. Dysregulation of miRNA could be a precursor to the dysregulation of genes, so it is important to identify what miRNAs are affected, and how PAHs directly affect the expression of miRNA via non-genotoxic pathways. Differential expression of miRNA has been observed in lung cancer (Yanaihara 2006) and other forms of cancer through multiple pathways including the dysregulation of transcription factors (O'Donnell 2005).

3D HBEC

This study investigated the role of miRNAs in regulating toxicity by PAHs in primary human bronchial epithelial cells (HBEC) cultured in 3D to mimic human response to exposure in vivo. The HBEC model contains functional human lung cells cultured in a monolayer that are airlifted to trigger differentiation of the cells, which form a pseudostratified 3D structure. This results in ciliated, goblet, and basal cells that produce mucus, and can move mucus and contaminants around in the culture well. This model more accurately reflects exposure at tissue interfaces, and supports metabolic activity as well as multicellular communication, which will provide a more dynamic response representative of cellular activity in vivo.

To evaluate whether miRNAs play a role in mediating toxicity by PAHs, interactions between experimentally observed miRNAs and genes were determined using Bioinformatics Resource Manager (BRM) followed by analysis in MetaCore to identify perturbed pathways and functionally classify miRNA relevant to PAH toxicity. This study is the first to describe the role of miRNA in mediating toxicity by PAHs in the human lung. Understanding the function of miRNA will help determine a more accurate mechanism of toxicity for BaP, DBC, and PAHs in general. Identification of miRNAs involved in PAH toxicity may progress their development as biomarkers

for early detection of toxicity and may also elucidate points of intervention for preventing toxicity by PAHs.

Materials and Methods

Chemicals and reagents.

Cell culture media and phosphate buffered saline (PBS) were provided by MatTek Corporation (Ashland, MA). Benzo[a]pyrene (CAS# 50-32-8) and dibenzo[def,p]chrysene (CAS# 189-64-0) were purchased from MRIGlobal (Kansas City, MO). DNase I, TRIzol® reagent, Superscript® III First Strand Synthesis System, qPCR primers, and Pierce™ LDH Cytotoxicity Assay Kit were from Thermo Fisher Scientific (Waltham, MA). 2X SsoAdvanced™ Universal SYBER®Green Supermix was purchased from BioRad Laboratories, Inc. (Hercules, CA.)

Tissue Culture and treatments.

EpiAirway™ 100 tissues were shipped overnight and received chilled on ice packs. Tissues were immediately transferred to 6-well plates each well containing 1 ml of assay medium. Tissues were then equilibrated for 24 hours at 37°C, 5% CO₂ followed by a change of fresh medium before any treatment regimens commenced. Initiation with PAHs was timed so that all treatments would be harvested on the same day thus all tissues would be cultured for the same number of days. Tissues were prepared for treatment as follows: PBS (0.50 ml) was pipetted onto the apical surface of the inserts and trans-epithelial resistance (TEER) was measured with an EVOM2 Epithelial Voltohmmeter, World Precision Instruments (Sarasota, FL.). The PBS was carefully removed along with mucus from the surface of the tissues. The medium was replaced with 1 ml of fresh medium in the plate wells (basal side of the membrane). Single PAHs and coal tar were solubilized in acetone and applied (0.01 ml/insert) to the apical surface of tissues by droplets using a pipette. BaP was dosed at 500 µg/µl and DBC at 10 µg/µl. Forty-eight hours post treatment, PBS (0.30ml) was added to the apical surface of each insert and TEER recorded. Apical washes and basal media were transferred to clean, sterile tubes and stored at -80°C. At the end of each exposure regimen, the matrix and

tissue from each well insert was carefully peeled away with forceps, placed in cryovials containing 0.5ml TRIzol® reagent and snap frozen in liquid nitrogen. Frozen tissues were stored at -80°C until further analysis.

Cell Viability.

MTT assays were used for measuring cell viability following MatTek's protocol. MTT reagent was diluted with the provided diluent. The diluted reagent (300µl) was placed in each well of a 24-well plate and equilibrated at 37°C. At the end of each treatment regimen a subsample of tissues from each group was washed on the apical side thrice with 0.4 ml PBS. All PBS was carefully aspirated away and inserts placed in wells containing warmed MTT reagent. The MTT assay plate was returned to 37°C, 5% CO₂ for 2 hours. MTT extraction solution (2.0 ml) was placed in wells of a clean 24-well plate. At the end of the 2 hr incubation, inserts were transferred into the extraction reagent, wrapped in foil, and shaken at room temperature for 2 hr. Aliquots of extraction solution were transferred to a 96-well plate. Optical density was determined at 570 nm and 650 nm (background subtraction) on a BioTek SYNERGY/HTX plate reader (Winooski, VT.)

Lactate Dehydrogenase Leakage.

Lactate dehydrogenase (LDH) leakage was measured in media from 6, 24, and 48 hr PAH exposed tissues. LDH leakage was measured with a Pierce LDH Cytotoxicity Assay Kit using the "Chemical Compound-Mediated Cytotoxicity" protocol. Reaction mixture was prepared per manufacturer's instructions by rehydrating lyophilized substrate mix with water and adding thawed assay buffer. Optimal absorbance output was determined by testing 10, 20, 30, 40, and 50 µl of media from acetone treated tissues and 40µl was chosen. Basal medium samples (40 µl) were aliquoted into the wells of a 96-well plate. LDH reaction reagent (40 µl) was added to each sample and incubated at room temperature for 30 minutes while protected from light.

Finally, 40 µl of stop solution was added to each well and mixed. LDH activity was determined by subtracting absorbance at 680 nm (background) from absorbance at 490 nm again using a SYNERGY/HTX reader. A negative control of fresh cell culture medium, a positive control of medium from lysed cells, and vehicle only controls were used in both assays.

RNA extraction and sequencing.

Total RNA was extracted from each sample well using TRIzol® reagent following published protocol for purification of total RNA from animal cells. Concentrations of RNA from samples were evaluated on a Synergy HTX Multi-Mode Microplate Reader using a Take3 Micro-Volume plate and pre-programmed Gen5 protocols for nucleic acid detection. Isolated RNA was submitted to the Oregon State University Center for Genome Research and Biocomputing for sequencing on Illumina HiSeq 3000 (OSU CGRB.)

Data Processing.

mRNA-Seq. Sequenced reads were first processed in Cutadapt version 1.8.1 (Martin, 2011) to trim adapter sequences from the paired-end reads. The human genome assembly GRCh38.p8 (<https://www.ncbi.nlm.nih.gov/assembly/>) was indexed using Bowtie2-build version 2.2.3 indexer (Langmead et al., 2012) while the transcriptome was indexed using TopHat version 2.1.1 (Trapnell et al., 2009.) TopHat was used again to align the trimmed reads to indexed transcriptome and genome. Differential expression was determined in CuffDiff version 2.2.1 (Trapnell et al., 2012.)

miRNA-Seq. Sequencing data from smallRNA-Seq was processed in Cutadapt to trim adapter sequences from single-end reads. The human genome assembly GRCh38.p8 was indexed using Bowtie-build for use with Bowtie version 0.12.9 (Langmead et al., 2009). The trimmed reads were aligned to the indexed reference genome using Bowtie using a seed length of 22 nucleotides with no more than two mismatches in the seed and reporting the best alignment to the output. The aligned reads were then run in featureCounts version 1.6.0 (Liao et

al., 2014) along with the gff3 annotation file from mirbase.org version 22 (Kozomara et al., 2014.) featureCounts was used to produce a count table for stem-loop and mature miRNA sequences. The count table produced by featureCounts was used in DESeq2 version 1.18.1 (Love et al., 2014) to calculate differential expression.

Reverse prediction analysis.

mRNA expression data was first used in Bioinformatic Resource Manager version 2.3 (Tilton et al., 2012.) to predict miRNA targeting significantly differentially expressed genes in the BaP or DBC data sets. These predicted miRNAs identified specific miRNA that are overconnected to gene in the dataset. This produced a list of miRNA to look for in the experimental dataset as well as processes that may be regulated directly by miRNA and may be unique to BaP or DBC. The workflow for miRNA prediction was similar to the workflow listed below for determining miRNA-mRNA interaction with the exception that miRNA expression data was not upload in BRM.

Determining miRNA-mRNA interactions.

miRNA-mRNA interactions were determined from experimental datasets using Bioinformatics Resource Manager. BRM uses three databases: Microcosm version 5 (Griffiths-Jones et al., 2008,) MicroRNA.org Release 8/2010 (Betel et al., 2008) and TargetScan version 7.1 (Agarwal et al., 2015) along with one experimentally validated database, miRTarBase version 6.1 (Chou et al., 2016) to make target predictions between experimental miRNA and mRNA. The miRNA and mRNA datasets were split up into BaP and DBC datasets, which were further split up into up- and down-regulated groups. The miRNAs significantly dysregulated in BaP and DBC were compared to identify miRNAs unique to BaP or DBC, and miRNAs common between the two treatments. Groups were formed for unique up-regulated and unique down-regulated miRNAs for each treatment as well as common up-regulated and common down-regulated miRNAs. Due to the inhibitory relationship between miRNA and mRNA, the datasets were submitted to BRM in an anti-correlated fashion. All target predictions containing hits in at

least one of the four databases were returned. The interactions were then filtered to hits that occurred in two or more databases, or a single hit in the miRTarBase database.

Process analysis.

Target genes, and their differential expression data, that met filtering criteria as listed above, were uploaded to MetaCore version 6.35 by Thompson Reuters (<http://www.genego.com/>) as datasets separated by treatment, unique or common regulation between treatments, and up- or down regulation. Gene in each dataset were analyzed using MetaCore's Functional Ontology Enrichment tool to identify perturbed biological processes.

Heatmap.

A heatmap of gene expression data was constructed for significant mature miRNA in MultiExperiment Viewer version 4.9.0 (Saeed et al., 2003). Hierarchical clustering was performed on the heat map under default settings in MeV.

miRNA-mRNA network construction.

Cytoscape version 3.6.1 (Shannon et al., 2003) was used to visualize the interactions between experimentally observed miRNA and mRNA transcripts. Separate interaction lists of previously filtered interactions were compiled for up- and down-regulated miRNA for each treatment. In Cytoscape this interaction list becomes a visual network of interactions, assigning each listed gene and miRNA to a node, interacting via edges. An attribute list was assembled for each network containing expression data and statistics for miRNA and genes, as well as processes each gene is involved in as determined by MetaCore. For clarity, genes present in the network were then filtered to only genes involved in the most significant processes. Nodes were arranged using the Edge-weighted Spring Embedded Layout algorithm included in Cytoscape. Nodes were then manually arranged to clarify grouping of perturbed processes

linked to each miRNA. Networks for up-regulated miRNA unique to BaP and DBC were merged to observe of regulation by different miRNA overlap for the two compounds.

Results

Predicted miRNA

The reverse prediction analysis identified five overconnected miRNAs targeting significant genes in the DBC group, miR-155-5p, -193a-3p, -212-3p, -328-3p, and -1301-3p. Seven overconnected miRNAs were identified in the BaP treatment group, miR-144-3p, -145-5p, -155-5p, -204-5p, -223-3p, 328-3p, and 1301-3p. The reverse predictions for BaP and DBC shared miR-155-5p, -328-3p, and -1301-3p. miR-145-5p was significant in the full analysis of the BaP group. miR-1301-3p was significant in the full analysis of the DBC group. miR-155-5p was the most overconnected miRNA in the reverse prediction, however it was not significantly differentially expressed. Regulation of Epithelial-to-Mesenchymal Transition, Extracellular Matrix Remodeling, and Glucocorticoid Receptor Signaling were the most significant processes targeted by predicted miRNAs.

Identifying Significantly Expressed miRNAs

The sequencing data for miRNA was processed and filtered for significance ($P < 0.05$.) BaP treatment contained 56 significantly differentially expressed mature miRNA while DBC contained 104 (Table 1.) The miRNA were split into up- and down- regulation to compare for identical miRNA between treatments. BaP and DBC shared seven up-regulated mature miRNAs, and one down-regulated miRNA. A heatmap was constructed in MeV for the miRNA expression data (Figure 1.)

Table 1. All miRNAs significantly differentially expressed in HBECs exposed to BaP or DBC

BaP Unique		Common		DBC Unique	
Up-regulated	Down-regulated	Up-regulated	Down-regulated	Up-regulated	Down-regulated
let-7c-5p, let-7d-3p, miR-10b-5p, miR-124-3p, miR-127-3p, miR-133a-3p, miR-139-5p, miR-143-3p, miR-143-5p, miR-145-3p, miR-145-5p, miR-148a-5p, miR-181a-3p, miR-183-3p, miR-184, miR-196a-5p, miR-196b-5p, miR-199a-3p, miR-199a-5p, miR-199b-3p, miR-214-3p, miR-27b-5p, miR-296-3p, miR-30b-5p, miR-3120-5p, miR-328-3p, miR-410-3p, miR-425-3p, miR-497-5p, miR-671-5p, miR-7974, miR-7977	miR-1307-5p, miR-2278, miR-23a-3p, miR-27a-5p, miR-324-5p, miR-3609, miR-3653-3p, miR-3653-5p, miR-4485-5p, miR-449c-5p, miR-532-5p, miR-6087, miR-664b-3p, miR-6723-5p	miR-149-5p, miR-150-5p, miR-221-3p, miR-30c-1-3p, miR-30c-5p, miR-671-3p, miR-1307-5p	miR-449b-5p	let-7b-3p, let-7b-5p, let-7e-5p, miR-1180-3p, miR-125a-3p, miR-125b-2-3p, miR-128-1-5p, miR-1301-3p, miR-1307-3p, miR-138-1-3p, miR-151a-3p, miR-181a-2-3p, miR-191-5p, miR-193a-5p, miR-23a-5p, miR-25-3p, miR-26b-3p, miR-30a-3p, miR-30c-2-3p, miR-30d-5p, miR-30e-3p, miR-3180-3p, miR-3184-3p, miR-3184-5p, miR-320a, miR-3605-3p, miR-423-3p, miR-423-5p, miR-455-3p, miR-486-3p, miR-486-5p, miR-500a-3p, miR-532-3p, miR-589-5p, miR-6510-3p, miR-6804-3p, miR-6812-3p, miR-744-5p, miR-877-5p, miR-92b-3p, miR-92b-5p, miR-941	let-7a-3p, miR-101-3p, miR-106b-5p, miR-122-5p, miR-135b-5p, miR-141-3p, miR-141-5p, miR-147b, miR-148b-5p, miR-153-3p, miR-15a-5p, miR-18a-5p, miR-200a-3p, miR-21-5p, miR-218-5p, miR-223-3p, miR-2467-5p, miR-26b-5p, miR-29a-3p, miR-29b-3p, miR-29c-3p, miR-301a-3p, miR-30d-3p, miR-30e-5p, miR-32-3p, miR-32-5p, miR-33a-5p, miR-33b-5p, miR-340-5p, miR-34b-5p, miR-34c-5p, miR-3591-3p, miR-3613-5p, miR-374a-3p, miR-374a-5p, miR-429, miR-449a, miR-450b-5p, miR-452-3p, miR-548e-3p, miR-548k, miR-561-5p, miR-582-3p, miR-582-5p, miR-590-3p, miR-598-3p, miR-651-5p, miR-660-5p, miR-708-3p, miR-944

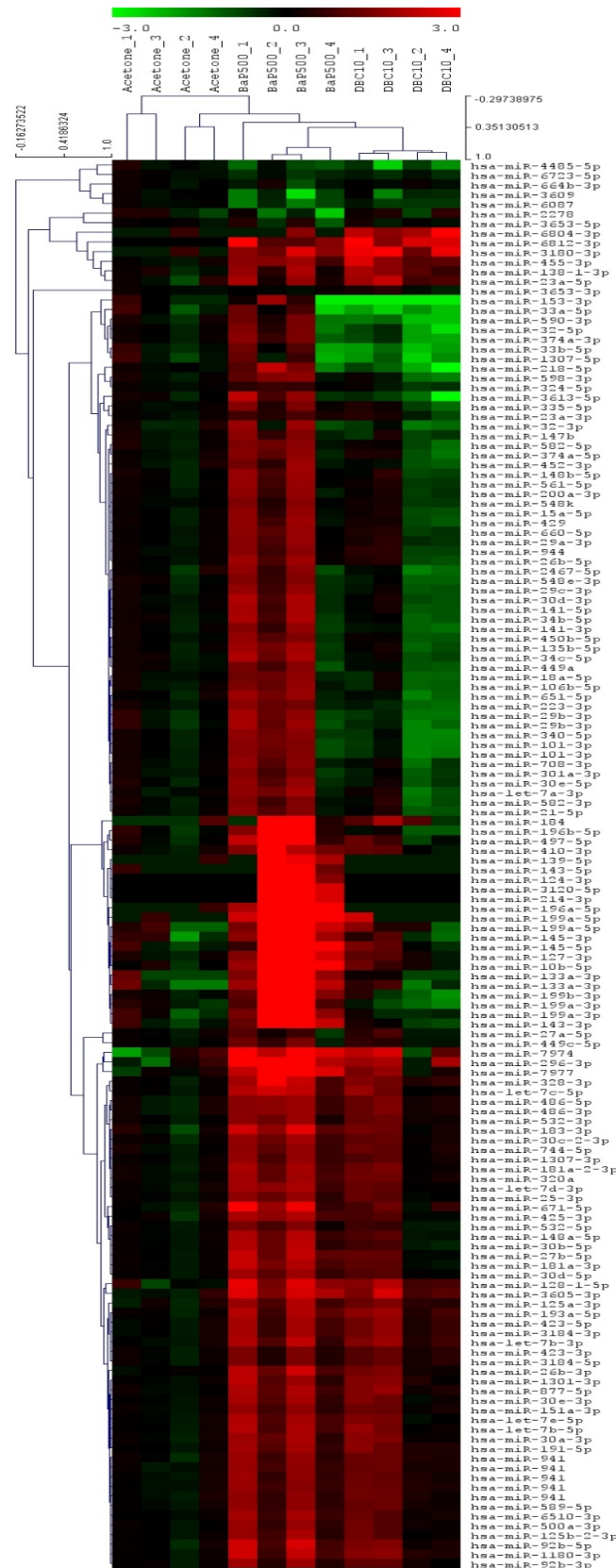


Fig. 1. A heatmap of expression counts for significant mature miRNA differentially expressed in BaP or DBC

miRNA-mRNA Integration

miRNA and mRNA datasets were integrated using Bioinformatics Resource Manager. In BaP, 11,952 miRNA-mRNA interactions were predicted for down-regulated miRNA and 85,332 for up-regulated miRNA. In DBC, 155,411 miRNA-mRNA interactions were predicted for down-regulated miRNA and 64,602 for up-regulated miRNA. Interactions were filtered to those which targeted genes from the experimental dataset. The interactions were then filtered for hits in two of four databases or miRTarBase. Filtering reduced the list of interactions for BaP down to 205 and 1,498 for down- and up-regulated miRNA respectively. In DBC interactions were reduced to 1,652 and 1,390 for down- and up-regulated miRNA respectively.

Process Analysis

Gene expression data for genes involved in the filtered interactions were submitted to MetaCore to determine

process networks that are perturbed by genes target by experimental miRNA. The perturbed processes were filtered for significance ($P < 0.05$) in either BaP or DBC. miRNA up-regulated in BaP appeared to be connected to genes involved with cell adhesion and developmental processes, and a weaker response in signal transduction processes. miRNA up-regulated in DBC showed a strong response for cell adhesion and development as well, but also showed significant responses in apoptosis, cell cycle, and translation processes (Figure 2.) BaP contained an average of 21 genes per significant process from the experimental dataset and DBC had an average of 19.

For down-regulated miRNA, significant processes were much fewer and spread across more categories with less significance. BaP showed perturbation in cytoskeletal and cell cycle processes, whereas DBC showed perturbation in cell cycle and DNA damage processes (Figure 3.) BaP showed an average of five genes from the dataset per significant process, and average of nine per significant process in DBC.

miRNA-mRNA Networks

Cytoscape was used to visual the networks of miRNA-mRNA interactions, focused on the most significant, differentially expressed miRNA that are overconnected to the most significant processes. The networks for up-regulated miRNA look at the top eight miRNA each in BaP and DBC. The BaP network contains 159 genes, while DBC contains 82. The BaP (Figure 4) network focuses on connections in processes of cell adhesion, development, and signal transduction. The DBC network (Figure 5) focuses on connections in processes of cell adhesion, development, and cell cycle. Each node in the networks was colored to denote involvement in a category of processes.



Figure 2. Processes significantly perturbed by experimental genes targeted by significant up-regulated miRNA. The P-value was log transformed and set at a level of 1.3 for significance.

Processes Perturbed by Down-Regulated miRNA

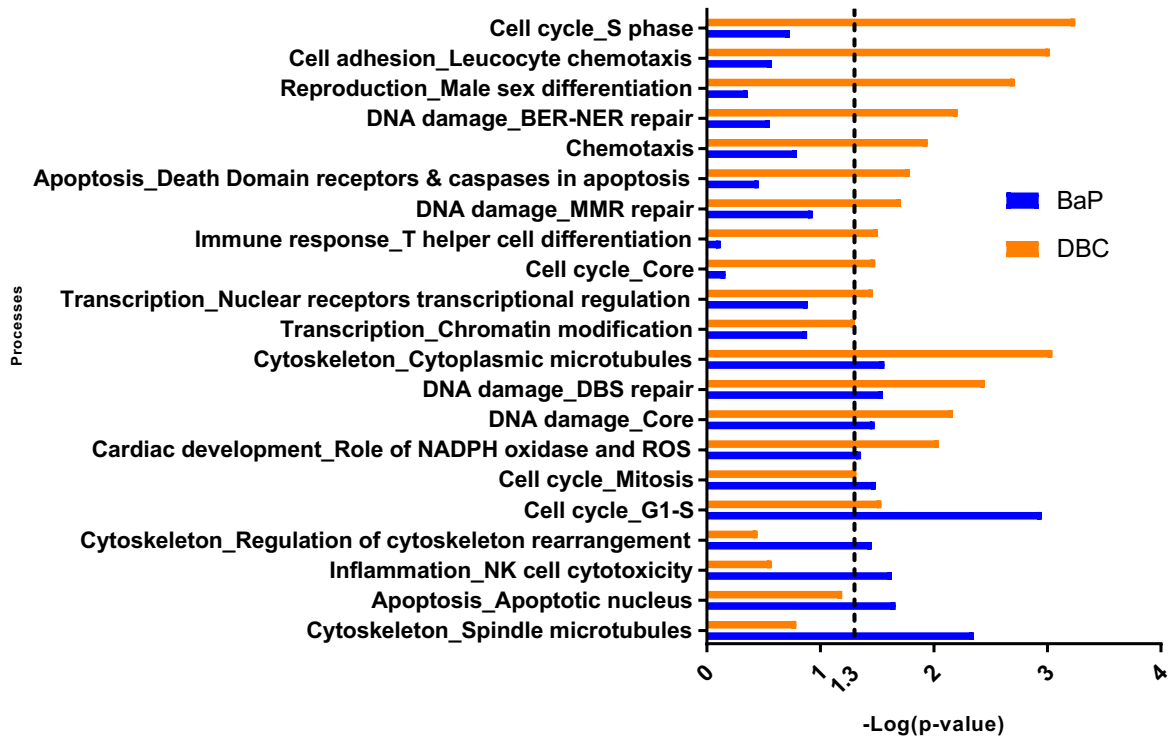


Figure 3. Processes significantly perturbed by experimental genes targeted by significant down-regulated miRNA. The P-value was log transformed and set at a level of 1.3 for significance.

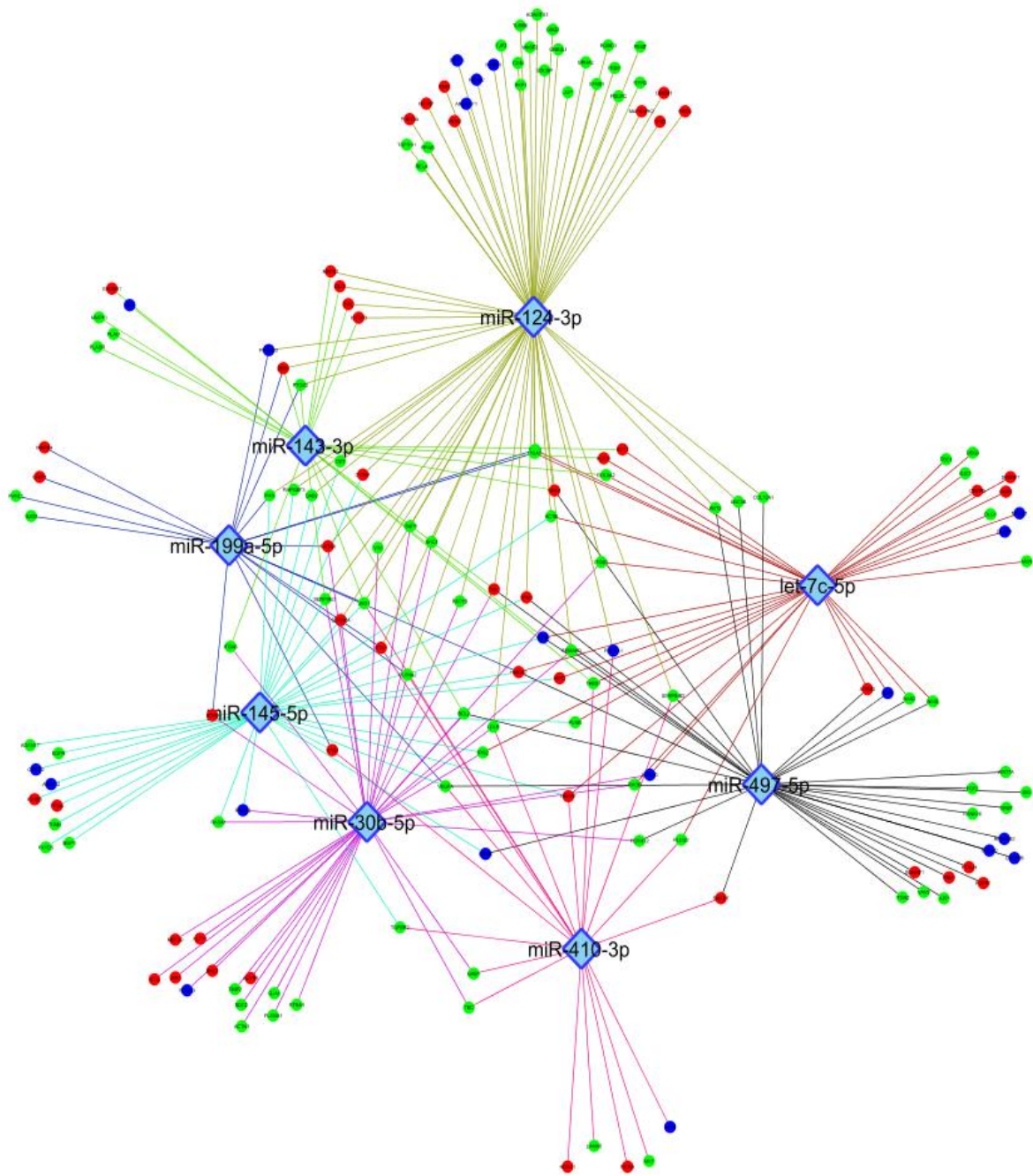


Figure 4. Network of up-regulated miRNA and down-regulated genes in BaP. Each circular node represents a gene, and the node color indicates the associated process; Green – Cell Adhesion, Red – Development, Blue – Signal Transduction. The color of the edge indicates the targeting miRNA.

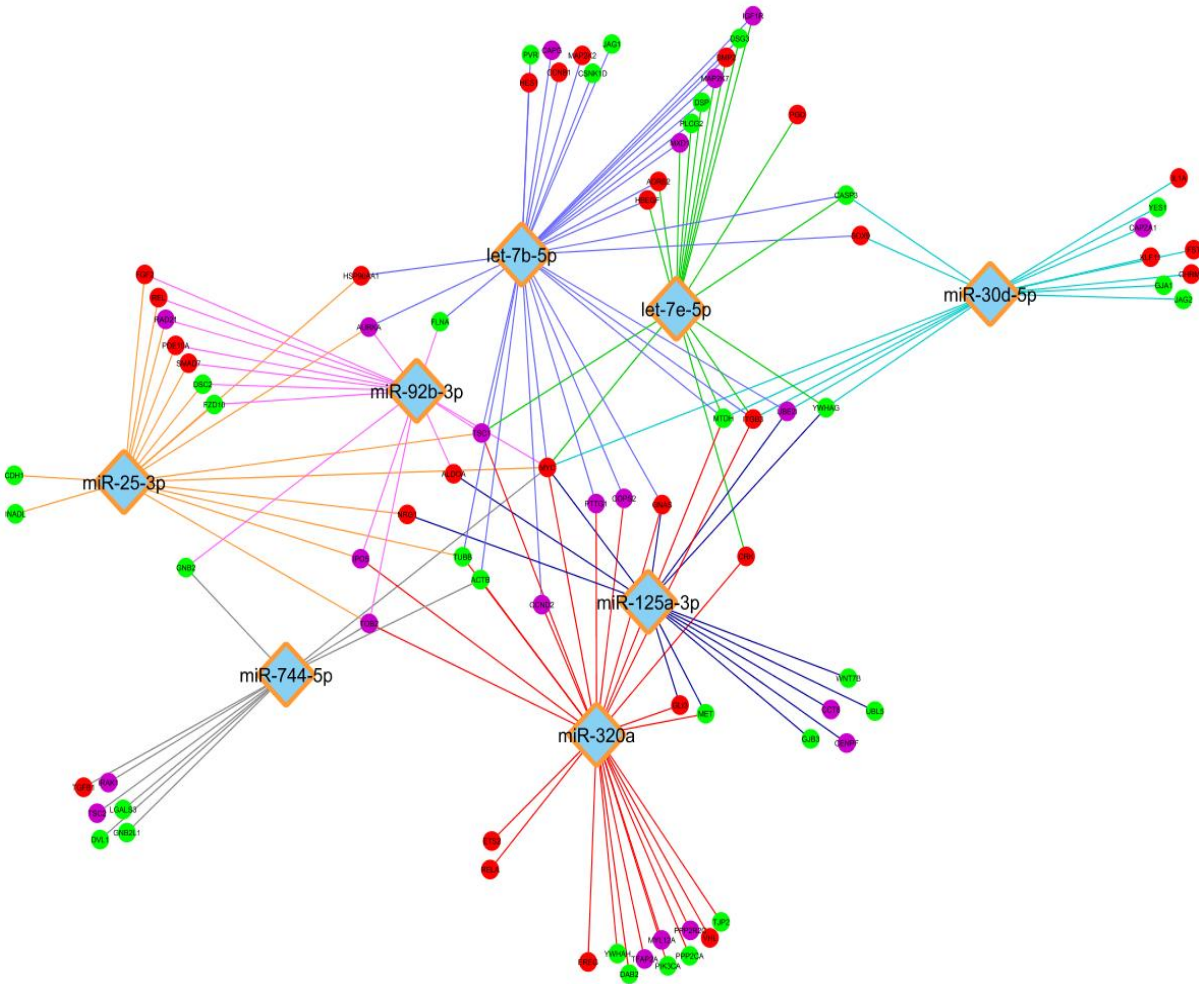


Figure 5. Network of up-regulated miRNA and down-regulated genes in DBC. Each circular node represents a gene, and the node color indicates the associated process; Green – Cell Adhesion, Red – Development, Purple – Cell Cycle. The color of the edge indicates the targeting miRNA.

Discussion

Polycyclic Aromatic Hydrocarbons are a class of chemically diverse contaminants that are ubiquitous throughout the environment. Many PAHs are procarcinogenic due to the structure of their rings. PAHs “bay” or “fjord” regions have been observed to be more reactive and are metabolized by the Cytochrome P450 enzymes to form diol epoxides which can cause direct damage to the DNA. Structurally different PAHs have been observed to have varying levels of potency as carcinogens. The difference in structure may influence carcinogenesis via non-genotoxic pathways. The role of miRNA has not yet been identified in PAH toxicity and is possibly a key regulator in mediating toxicity by PAHs in human bronchial epithelial cells which may explain differences in potency and unique mechanisms of carcinogenesis. This study aims to identify aberrantly expressed miRNA and functionally classify them by expression patterns in their target genes to determine miRNAs involved in mediating PAH toxicity.

miRNA are important post-transcriptional regulator molecules involved in maintaining normal gene expression and mediating cellular response. The dysregulation of miRNA has been identified in the development of non-small cell lung cancer in response to cigarette smoke (Babu et al. 2018.) PAHs such as BaP interact with the aryl hydrocarbon receptor (AhR,) initiating transcription of many gene including genes for the metabolism. The vast class of PAHs features many different conformations of two or more benzene rings which may influence the affinity of the compound for certain receptors in the cell or nuclear membrane, or response elements following translocation into the nucleus. Off-target interaction with receptors may induce expression of miRNA as a response to mediate the effect of PAH exposure and subsequent genotoxic damage. Identification of miRNAs involved in toxicity may help develop them as biomarkers of toxicity for PAH exposure and aid in the identification of points of intervention for PAH toxicity.

Benzo(a)pyrene is a well-studied carcinogen, often used as a benchmark for PAH studies. The potencies of PAHs are measured through in vivo dermal toxicity studies in mice and are used to rank PAHs by potency relative to BaP, known as the relative potency factor. DBC is approximately fifty times more potent than BaP. A 3D human bronchial epithelial model was used because it is representative of the lung. The model contains functional human lung cells cultured in a monolayer that are then airlifted to trigger differentiation of the cells which form a 3D structure. miRNA-gene relationships were identified using Bioinformatic Resource Manager to integrate mRNA and miRNA sequencing data from the HBE cells based on known and experimental targets for miRNA.

Differentially Expressed miRNA Unique to BaP

The miRNA that were most significantly and uniquely up-regulated by BaP were strongly associated with processes involved in cell adhesion, development, and signal transduction. There were also abundant, but less significant, interactions with genes in cytoskeletal and proliferation processes. miR-124-3p was the most overconnected miRNA in the BaP dataset, it primarily connected to genes involved in cell adhesion and development processes. miR-124 has been identified in non-small cell lung cancer (NSCLC) as a potential biomarker of prognosis and tumor response to chemotherapy. It is also involved with tumor suppression in multiple forms of cancer including lung and breast cancer (Luo et al. 2017.)

miR-30b-5p, miR-497-5p, miR-145-5p, miR-143-3p, and let-7c-5p were also highly connected to genes down regulated in BaP treatments, but connected to about half as many significant process-related genes as miR-124-3p. Previous studies have identified miR-30b as an inhibitor of cell proliferation in NSCLC and down-regulation of miR-30b is associated with tumor differentiation and metastatic stages of NSCLC (Chen et al. 2015.) miR-497-5p strongly connected to developmental pathways and down-regulation of miR-497 has been identified in

many forms of cancer, and targets several genes in the dataset involved in tumorigenesis such as *BCL-2*, *VEGF-A*, *IGF1R*, and *SMURF1* (Yang et al. 2016.) Overexpression of miR-145-5p has been observed suppressing the epithelial-to-mesenchymal transition (EMT) in esophageal squamous cell carcinoma (ESCC) by regulation of the nuclear factor kB (NF-kB) signaling pathways. miR-145 was observed in the dataset regulating gene *MMP2* and *MMP13*, both of which are present in the breakdown of extracellular matrix and tissue remodeling, and involved with EMT (Mei et al. 2017.) Regulation of EMT is one of the most significant processes for miR-145-5p in the BaP dataset, and the process is significant among the other major miRNA excluding miR-30b-5p. Up-regulation of miR-143-3p has been observed to down-regulate *MAPK7*, inhibiting cell proliferation and migration in breast cancer (Xia et al. 2018.) The interaction between *MAPK7* and miR-143 was present in the BaP dataset. The miRNA let-7c-5p was observed to be more strongly involved in processes of signal transductions than other major miRNAs except for miR-124-3p. let-7c-3p is known to be involved in a positive feedback loop in HBE cells exposed to cigarette smoke extract which contains PAHs in mixture. This feedback loop involves the gene *c-Myc* and long non-coding RNA CCAT1. let-7c ordinarily down-regulates *c-Myc*, however CCAT1 acts as a sponge for let-7c, preventing the down-regulation of *c-Myc*. Overexpression of *c-Myc* is necessary for the up-regulation of proliferation process (Lu et al. 2017.)

The above miRNA were all identified as having some tumor suppressive gene targets in multiple forms of cancer, however in those conditions the miRNA were down-regulated leading to the development of cancer. In the HBE cells treated with BaP, these miRNA were significantly up-regulated which may indicate non-genotoxic effects of PAH that promotes a regulatory response in the cells.

Differentially Expressed miRNA Unique to DBC

The DBC treatment group showed more miRNAs significantly up-regulated than the BaP group, however they did not connect to processes as definitively making it difficult to classify

miRNA. Overall DBC miRNAs differentially expressed in response to DBC connected most to cell adhesion and development processes, as seen in BaP, as well as cell cycle processes. The miRNA let-7b-5p was the most overconnected miRNA in the DBC network, primarily connecting to genes associated with development, and targets IGF1R to regulate cell proliferation and cell death multiple myeloma (Xu et al. 2014.) The interaction between let-7b and IGF1R was also observed in the HBE cells treated with DBC. Let-7e-5p has been identified as a potential biomarker of prognosis for NSCLC alongside miR-125a-5p (Zhu et al. 2014) which was also differentially expressed in the DBC treatment group. Both miRNA along with miR-99b have been identified as part of the same cluster of miRNA, overexpression of this cluster promotes cell migration and metastasis in cancers such as ESCC (Ma et al. 2017.) As with let-7b in DBC, and miR-497 in BaP, *IGF1R* is a known target of miR-320a and can be observed in the DBC network. miR-320a is known to suppress tumor growth through IGF1R in NSCLC (Wang et al. 2017.) In the DBC network miR-320a was most connected to genes associated with development. The miR-30 family has broadly been classified as pro-oncogenic in multiple cancer types. However, in NSCLC miR-30a and miR-30d were observed to play a protective role by preventing tumor growth (Chen et al. 2015.) miR-30d-5p was significantly up-regulated in DBC treatments. miR-92b-3p directly targets gene *ITGA6* in the DBC network and the interaction has been associated with suppression of cell motility in ESCC, as *ITGA6* promotes motility and invasion in ESCC (Ma et al. 2017.)

Comparison of Networks

The present study examined miRNA that were uniquely differentially expressed in HBE cells treated with either BaP or DBC. Among broad categories, miRNAs uniquely up-regulated in BaP targeted genes most commonly associated with cell adhesion, development and, to a lesser extent, signal transduction. miRNAs uniquely up-regulated by DBC also predominately targeted genes associated with cell adhesion and development, but also strongly connected with cell cycle processes. DBC overall contained more significant miRNA, however the miRNA

contained fewer gene targets across the dataset making it difficult to confidently classify miRNA by function.

Limitations

This study examined the role miRNA play in mediating toxicity by BaP or DBC in HBE cells. The PAHs test were used in isolation; however, in the environment PAHs are found in complex mixtures which may modulate the behavior and potency of the PAH. miRNA were only measured at one time point and for a single dose of BaP or DBC. Literature for the miRNAs identified indicated that they were down-regulated in most tumors. By only using the 48 hour timepoint, only the initial response was measured. Measuring miRNA across multiple timepoints would depict how miRNA response changes, and influences gene expression, over time following exposure. This study looks at a single exposure, as opposed to chronic exposure observed in vivo, so conclusions on the long-term role of miRNAs in mediating toxicity by PAHs cannot be determined. The different doses were selected to provide equivalent potencies when dosing BaP and DBC, DBC was smaller by a factor of 50. This smaller dose may have influenced the amount of DBC absorbed by the cells relative to the amount of BaP absorbed. The cells were dosed in plastic wells, so deposition of the PAH onto the walls of the well may impact DBC dosing more than BaP dosing.

Future Directions

Continual analysis of current data will look at more specific processes to classify miRNA and processes that are similarly regulated by BaP and DBC through unique miRNA. Future analysis will also examine miRNA potentially down-regulated by BaP or DBC, allowing the overexpression of genes down-stream. Relevant miRNA have been determined from the miRNA and mRNA data provided, however the miRNA still need to be confirmed, and their function investigated further. The presence of the miRNA can be confirmed by real-time qPCR to ensure the miRNAs identified are being differentially expressed as a result of PAH treatment. Following confirmation, the function of miRNAs can be observed through knockout experiments in which

the expression of a single miRNA is eliminated. This will allow target genes to be experimentally identified, and processes to be more confidently tied to miRNA through the differentially expressed genes. Continual analysis of current data will look at more specific processes to classify miRNA and processes that are similarly regulated by BaP and DBC through unique miRNA. Future analysis will also examine miRNA potentially down-regulated by BaP or DBC, allowing the overexpression of genes down-stream. Future experiments may also examine the role of miRNA in response to complex mixtures PAHs, as well as the role of lncRNAs regulating miRNA expression.

This study has identified differentially expressed miRNA in HBE cells treat by either BaP or DBC. miRNAs likely play a role in mediating toxicity by PAHs and preventing development of a carcinogenic state. The miRNAs identified need further investigation to better understand their function in the cell. The presence of differentially expressed miRNA, as well as specific interactions, in both the experimental data and literature for many forms of cancer confirm that these miRNAs do play a role in carcinogenesis and therefore carcinogenic PAHs as well. Determining the functional role of miRNA in mediating toxicity by PAHs will help refine the mechanism of toxicity for PAHS by identifying associated non-genotoxic effects. These non-genotoxic effects may be helpful in primary screening of PAHs for toxicity testing and miRNAs may also be developed as biomarkers of toxic exposure to PAHs.

References

- Agarwal V, Bell GW, Nam J-W, Bartel DP. 2015 Aug 12. Predicting effective microRNA target sites in mammalian mRNAs. *eLife*. doi:[10.7554/eLife.05005](https://doi.org/10.7554/eLife.05005). [accessed 2018 Aug 21]. <https://elifesciences.org/articles/05005>.
- Agency for Toxic Substances and Disease Registry (ATSDR). 1995. Toxicological profile for Polycyclic Aromatic Hydrocarbons (PAHs). Atlanta, GA: U.S. Department of Health and Human Services, Public Health Service.
- Agency for Toxic Substances and Disease Registry (ATSDR). 2005. Toxicological profile for Naphthalene, 1-Methylnaphthalene, and 2-Methylnaphthalene. Atlanta, GA: U.S. Department of Health and Human Services, Public Health Service.
- Babu N, Advani J, Solanki HS, Patel K, Jain A, Khan AA, Radhakrishnan A, Sahasrabudhe NA, Mathur PP, Nair B, et al. 2018 Mar 31. miRNA and proteomic dysregulation in non-small cell lung cancer in response to cigarette smoke. *MicroRNA*. [accessed 2018 Sep 5]. <http://www.eurekaselect.com/158809/article>.
- Betel D, Wilson M, Gabow A, Marks DS, Sander C. 2008. The microRNA.org resource: targets and expression. *Nucleic Acids Res*. 36(Database issue):D149–D153. doi:[10.1093/nar/gkm995](https://doi.org/10.1093/nar/gkm995).
- Chen D, Guo W, Qiu Z, Wang Q, Li Y, Liang L, Liu L, Huang S, Zhao Y, He X. 2015. MicroRNA-30d-5p inhibits tumour cell proliferation and motility by directly targeting CCNE2 in non-small cell lung cancer. *Cancer Lett*. 362(2):208–217. doi:[10.1016/j.canlet.2015.03.041](https://doi.org/10.1016/j.canlet.2015.03.041).
- Chen H, Pan H, Qian Y, Zhou W, Liu X. 2018. MiR-25-3p promotes the proliferation of triple negative breast cancer by targeting BTG2. *Mol Cancer*. 17. doi:[10.1186/s12943-017-0754-0](https://doi.org/10.1186/s12943-017-0754-0). [accessed 2018 Sep 5]. <https://www.ncbi.nlm.nih.gov/pmc/articles/PMC5759260/>.
- Chen S, Li P, Yang R, Cheng R, Zhang F, Wang Y, Chen X, Sun Q, Zang W, Du Y, et al. 2015. microRNA-30b inhibits cell invasion and migration through targeting collagen triple helix repeat containing 1 in non-small cell lung cancer. *Cancer Cell Int*. 15(1):85. doi:[10.1186/s12935-015-0236-7](https://doi.org/10.1186/s12935-015-0236-7).
- Chou C-H, Chang N-W, Shrestha S, Hsu S-D, Lin Y-L, Lee W-H, Yang C-D, Hong H-C, Wei T-Y, Tu S-J, et al. 2016. miRTarBase 2016: updates to the experimentally validated miRNA-target interactions database. *Nucleic Acids Res*. 44(Database issue):D239–D247. doi:[10.1093/nar/gkv1258](https://doi.org/10.1093/nar/gkv1258).
- Griffiths-Jones S, Saini HK, van Dongen S, Enright AJ. 2008. miRBase: tools for microRNA genomics. *Nucleic Acids Res*. 36(Database issue):D154–D158. doi:[10.1093/nar/gkm952](https://doi.org/10.1093/nar/gkm952).
- Harper TA, Morr e J, Lauer FT, McQuistan TJ, Hummel JM, Burchiel SW, Williams DE. 2015. Analysis of Dibenzo[def,p]chrysene-deoxyadenosine adducts in wild-type and cytochrome P450 1b1 knockout mice using stable-isotope dilution UHPLC-MS/MS. *Mutat Res Genet Toxicol Environ Mutagen*. 782:51–56. doi:[10.1016/j.mrgentox.2015.03.007](https://doi.org/10.1016/j.mrgentox.2015.03.007).
- Kozomara A, Griffiths-Jones S. 2014. miRBase: annotating high confidence microRNAs using deep sequencing data. *Nucleic Acids Res*. 42(Database issue):D68–D73. doi:[10.1093/nar/gkt1181](https://doi.org/10.1093/nar/gkt1181).
- Langmead B, Salzberg SL. 2012. Fast gapped-read alignment with Bowtie 2. *Nature Methods*. 9(4):357–359. doi:[10.1038/nmeth.1923](https://doi.org/10.1038/nmeth.1923).

- Langmead B, Trapnell C, Pop M, Salzberg SL. 2009. Ultrafast and memory-efficient alignment of short DNA sequences to the human genome. *Genome Biology*. 10(3):R25. doi:[10.1186/gb-2009-10-3-r25](https://doi.org/10.1186/gb-2009-10-3-r25).
- Liao Y, Smyth GK, Shi W. 2014. featureCounts: an efficient general purpose program for assigning sequence reads to genomic features. *Bioinformatics*. 30(7):923–930. doi:[10.1093/bioinformatics/btt656](https://doi.org/10.1093/bioinformatics/btt656).
- Love MI, Huber W, Anders S. 2014. Moderated estimation of fold change and dispersion for RNA-seq data with DESeq2. *Genome Biology*. 15(12):550. doi:[10.1186/s13059-014-0550-8](https://doi.org/10.1186/s13059-014-0550-8).
- Lu L, Qi H, Luo F, Xu H, Ling M, Qin Y, Yang P, Liu X, Yang Q, Xue J, et al. 2017. Feedback circuitry via let-7c between lncRNA CCAT1 and c-Myc is involved in cigarette smoke extract-induced malignant transformation of HBE cells. *Oncotarget*. 8(12):19285–19297. doi:[10.18632/oncotarget.15195](https://doi.org/10.18632/oncotarget.15195).
- Luo P, Yang Q, Cong L-L, Wang X-F, Li Y-S, Zhong X-M, Xie R-T, Jia C-Y, Yang H-Q, Li W-P, et al. 2017. Identification of miR-124a as a novel diagnostic and prognostic biomarker in non-small cell lung cancer for chemotherapy. *Mol Med Rep*. 16(1):238–246. doi:[10.3892/mmr.2017.6595](https://doi.org/10.3892/mmr.2017.6595).
- Ma G, Jing C, Huang F, Li X, Cao X, Liu Z. 2017. Integrin $\alpha 6$ promotes esophageal cancer metastasis and is targeted by miR-92b. *Oncotarget*. 8(4):6681–6690. doi:[10.18632/oncotarget.14259](https://doi.org/10.18632/oncotarget.14259).
- Ma J, Zhan Y, Xu Z, Li Y, Luo A, Ding F, Cao X, Chen H, Liu Z. 2017. ZEB1 induced miR-99b/let-7e/miR-125a cluster promotes invasion and metastasis in esophageal squamous cell carcinoma. *Cancer Lett*. 398:37–45. doi:[10.1016/j.canlet.2017.04.006](https://doi.org/10.1016/j.canlet.2017.04.006).
- Martin M. 2011. Cutadapt removes adapter sequences from high-throughput sequencing reads. *EMBnet.journal*. 17(1):10–12.
- Mei L-L, Wang W-J, Qiu Y-T, Xie X-F, Bai J, Shi Z-Z. 2017. miR-145-5p suppresses tumor cell migration, invasion and epithelial to mesenchymal transition by regulating the Sp1/NF- κ B signaling pathway in esophageal squamous cell carcinoma. *Int J Mol Sci*. 18(9). doi:[10.3390/ijms18091833](https://doi.org/10.3390/ijms18091833).
- O'Donnell KA, Wentzel EA, Zeller KI, Dang CV, Mendell JT. 2005. c-Myc-regulated microRNAs modulate E2F1 expression. *Nature*. 435(7043):839–843. doi:[10.1038/nature03677](https://doi.org/10.1038/nature03677).
- Saeed AI, Sharov V, White J, Li J, Liang W, Bhagabati N, Braisted J, Klapa M, Currier T, Thiagarajan M, et al. 2003. TM4: a free, open-source system for microarray data management and analysis. *BioTechniques*. 34(2):374–378.
- Shannon P, Markiel A, Ozier O, Baliga NS, Wang JT, Ramage D, Amin N, Schwikowski B, Ideker T. 2003. Cytoscape: A software environment for integrated models of biomolecular interaction networks. *Genome Res*. 13(11):2498–2504. doi:[10.1101/gr.1239303](https://doi.org/10.1101/gr.1239303).
- Siegel RL, Miller KD, Jemal A. 2017. Cancer statistics, 2017. *CA: A Cancer Journal for Clinicians*. 67(1):7–30. doi:[10.3322/caac.21387](https://doi.org/10.3322/caac.21387).
- Tilton SC, Tal TL, Scroggins SM, Franzosa JA, Peterson ES, Tanguay RL, Waters KM. 2012. Bioinformatics resource manager v2.3: an integrated software environment for systems biology with microRNA and cross-species analysis tools. *BMC Bioinformatics*. 13(1):311. doi:[10.1186/1471-2105-13-311](https://doi.org/10.1186/1471-2105-13-311).

- Trapnell C, Pachter L, Salzberg SL. 2009. TopHat: discovering splice junctions with RNA-Seq. *Bioinformatics*. 25(9):1105–1111. doi:[10.1093/bioinformatics/btp120](https://doi.org/10.1093/bioinformatics/btp120).
- Trapnell C, Roberts A, Goff L, Pertea G, Kim D, Kelley DR, Pimentel H, Salzberg SL, Rinn JL, Pachter L. 2012. Differential gene and transcript expression analysis of RNA-seq experiments with TopHat and Cufflinks. *Nature Protocols*. 7(3):562–578. doi:[10.1038/nprot.2012.016](https://doi.org/10.1038/nprot.2012.016).
- Vu T, Jin L, Datta PK. 2016. Effect of cigarette smoking on epithelial to mesenchymal transition (EMT) in lung cancer. *J Clin Med*. 5(4). doi:[10.3390/jcm5040044](https://doi.org/10.3390/jcm5040044). [accessed 2018 Sep 6]. <https://www.ncbi.nlm.nih.gov/pmc/articles/PMC4850467/>.
- Wang Jianguo, Shi C, Wang Jianfei, Cao L, Zhong L, Wang D. 2017. MicroRNA-320a is downregulated in non-small cell lung cancer and suppresses tumor cell growth and invasion by directly targeting insulin-like growth factor 1 receptor. *Oncol Lett*. 13(5):3247–3252. doi:[10.3892/ol.2017.5863](https://doi.org/10.3892/ol.2017.5863).
- Xia C, Yang Y, Kong F, Kong Q, Shan C. 2018. MiR-143-3p inhibits the proliferation, cell migration and invasion of human breast cancer cells by modulating the expression of MAPK7. *Biochimie*. 147:98–104. doi:[10.1016/j.biochi.2018.01.003](https://doi.org/10.1016/j.biochi.2018.01.003).
- Xu H, Liu C, Zhang Y, Guo X, Liu Z, Luo Z, Chang Y, Liu S, Sun Z, Wang X. 2014. Let-7b-5p regulates proliferation and apoptosis in multiple myeloma by targeting IGF1R. *Acta Biochim Biophys Sin (Shanghai)*. 46(11):965–972. doi:[10.1093/abbs/gmu089](https://doi.org/10.1093/abbs/gmu089).
- Yanaihara N, Caplen N, Bowman E, Seike M, Kumamoto K, Yi M, Stephens RM, Okamoto A, Yokota J, Tanaka T, et al. 2006. Unique microRNA molecular profiles in lung cancer diagnosis and prognosis. *Cancer Cell*. 9(3):189–198. doi:[10.1016/j.ccr.2006.01.025](https://doi.org/10.1016/j.ccr.2006.01.025).
- Yang G, Xiong G, Cao Z, Zheng S, You L, Zhang T, Zhao Y. 2016. miR-497 expression, function and clinical application in cancer. *Oncotarget*. 7(34):55900–55911. doi:[10.18632/oncotarget.10152](https://doi.org/10.18632/oncotarget.10152).
- Yang S-J, Yang S-Y, Wang D-D, Chen X, Shen H-Y, Zhang X-H, Zhong S-L, Tang J-H, Zhao J-H. 2017. The miR-30 family: Versatile players in breast cancer. *Tumor Biology*. 39(3):101042831769220. doi:[10.1177/1010428317692204](https://doi.org/10.1177/1010428317692204).
- Zhu W-Y, Luo B, An J-Y, He J-Y, Chen D-D, Xu L-Y, Huang Y-Y, Liu X-G, Le H-B, Zhang Y-K. 2014. Differential expression of miR-125a-5p and let-7e predicts the progression and prognosis of non-small cell lung cancer. *Cancer Invest*. 32(8):394–401. doi:[10.3109/07357907.2014.922569](https://doi.org/10.3109/07357907.2014.922569).